Long-term population spike-timing-dependent plasticity promotes synaptic tagging but not cross-tagging in rat hippocampal area CA1

Karen Ka Lam Pang[a,b], Mahima Sharma[a,b,c,1], Kumar Krishna-K.[a,b,1], Thomas Behnisch[d,2], and Sreedharan Sajikumar[a,b,2]

[a]Department of Physiology, National University of Singapore, Singapore 117593; [b]Neurobiology/Aging Programme, Life Sciences Institute, Centre for Life Sciences, National University of Singapore, Singapore 117456; [c]Department of Biomedical Engineering, City College of New York, New York, NY 10031; and [d]Institutes of Brain Science, State Key Laboratory of Medical Neurobiology, Ministry of Education Frontiers Centre for Brain Science, Fudan University, Shanghai 200032, People's Republic of China

Edited by Mu-ming Poo, Chinese Academy of Sciences, Shanghai, China, and approved February 6, 2019 (received for review October 12, 2018)

In spike-timing-dependent plasticity (STDP), the direction and degree of synaptic modification are determined by the coherence of pre- and postsynaptic activities within a neuron. However, in the adult rat hippocampus, it remains unclear whether STDP-like mechanisms in a neuronal population induce synaptic potentiation of a long duration. Thus, we asked whether the magnitude and maintenance of synaptic plasticity in a population of CA1 neurons differ as a function of the temporal order and interval between pre- and postsynaptic activities. Modulation of the relative timing of Schaffer collateral fibers (presynaptic component) and CA1 axons (postsynaptic component) stimulations resulted in an asymmetric population STDP (pSTDP). The resulting potentiation in response to 20 pairings at 1 Hz was largest in magnitude and most persistent (4 h) when presynaptic activity coincided with or preceded postsynaptic activity. Interestingly, when postsynaptic activation preceded presynaptic stimulation by 20 ms, an immediate increase in field excitatory postsynaptic potentials was observed, but it eventually transformed into a synaptic depression. Furthermore, pSTDP engaged in selective forms of late-associative activity: It facilitated the maintenance of tetanization-induced early long-term potentiation (LTP) in neighboring synapses but not early long-term depression, reflecting possible mechanistic differences with classical tetanization-induced LTP. The data demonstrate that a pairing of pre- and postsynaptic activities in a neuronal population can greatly reduce the required number of synaptic plasticity-evoking events and induce a potentiation of a degree and duration similar to that with repeated tetanization. Thus, pSTDP determines synaptic efficacy in the hippocampal CA3–CA1 circuit and could bias the CA1 neuronal population toward potentiation in future events.

STDP | synaptic tagging | synaptic capture | area CA1 | synaptic plasticity

It is widely accepted that learning and memory are subserved by long-term modifications of synaptic efficacy in neural circuits (1). The most studied forms of such synaptic plasticity include long-term potentiation (LTP) and long-term depression (LTD). Both LTP and LTD are dissociated into different temporal phases (early LTP or LTD and late LTP or LTD) that are governed by distinct but related molecular mechanisms (2–4). The induction of both LTP and LTD is mediated by the dynamics of postsynaptic calcium influx and calcium-dependent signaling cascades (2, 5, 6). Furthermore, cellular consolidation of LTP and LTD is also determined by other neural activities occurring near the time of induction, as outlined by the synaptic tagging and capture (STC) hypothesis (7–9). The STC hypothesis points out that a strong activation (e.g., strong tetanization) of synapses potentiates those synapses by a dual mechanism—setting synapse-specific "tags" and triggering the synthesis of plasticity-related products (PRPs). In addition, other synapses that form a synaptic tag but express a transient synaptic potentiation (early LTP) due to a weak tetanization can capture and utilize the previously formed PRPs to stabilize their potentiation. The STC phenomenon has not only been observed in synapses expressing plasticity of the same polarity but also in synapses expressing opposing directions of change. In a phenomenon termed "cross-tagging," LTP and LTD positively interact, such that translation-dependent late LTP or late LTD reinforces translation-independent early LTD or LTP on neighboring synapses, respectively (3, 10, 11). The STC hypothesis highlights the fact that synaptic efficacy is shaped by neural activity occurring on a multitude of time scales (9).

Timing lies at the core of another subject of study of Hebbian plasticity—spike-timing-dependent plasticity (STDP). In STDP, the critical determinants of synaptic plasticity induction are the order of and relative timing between pre- and postsynaptic action potentials. Commonly, potentiation ensues when presynaptic activities repeatedly precede postsynaptic backpropagating action potentials within tens of milliseconds; conversely, depression results when synaptic transmission follows postsynaptic spikes (12, 13).

Studies of STDP in the hippocampus have described a variety of STDP curves with varying potentiation and depression windows depending on the experimental conditions (13–18). These STDP curves delineate changes in synaptic efficacy observed immediately after STDP induction (typically <20 min after induction). To our knowledge, no one has yet systematically investigated whether spike-timing-dependent potentiation or depression results in a synaptic change that lasts several hours. Previous studies of

Significance

Deciphering the rules that shape neuronal connections is critical to our understanding of information processing in a neural network. Our study describes how the relative timing of the activities of afferents and their associated postsynaptic neurons determines synaptic strength at the hippocampal CA1 circuit, an area important for learning and memory. A low number of repeated, paired activities between afferents and their neurons differentially shapes the hippocampal CA3–CA1 synaptic pathway for hours and even affects how future information is processed in the neuronal ensemble.

Author contributions: K.K.L.P., M.S., K.K.-K., T.B., and S.S. designed research; K.K.L.P., M.S., K.K.-K., T.B., and S.S. performed research; K.K.L.P., M.S., K.K.-K., T.B., and S.S. analyzed data; and K.K.L.P., M.S., T.B., and S.S. wrote the paper.

The authors declare no conflict of interest.

This article is a PNAS Direct Submission.

[1]M.S. and K.K.-K. contributed equally to this work.

[2]To whom correspondence may be addressed. Email: behnish@fudan.edu.cn or phssks@nus.edu.sg.

This article contains supporting information online at www.pnas.org/lookup/suppl/doi:10.1073/pnas.1817643116/-/DCSupplemental.

STDP relied on whole-cell voltage-clamp recordings that do not permit the recording of synaptic events for many hours as with field recordings. As mentioned, conventional tetanization-induced LTP and LTD are shown to display distinguishable phases over the course of its construction. Given that STDP has been theorized to constitute the basis of synaptic modification, it is fair to assume that STDP shares common induction and maintenance mechanisms with classical LTP and LTD. Empirical evidence supports the notion that spiking patterns modulate calcium transients in the postsynaptic cell and hence determine the polarity and degree of synaptic change (17, 19). By the same token, it seems plausible that these timing-dependent dynamics of calcium flux could lead to differential activation of downstream signaling cascades governing the long-term maintenance of such synaptic modifications, similar to that in tetanization-induced early LTP and late LTP. Therefore, we hypothesize that the persistence, in addition to the direction and magnitude, of STDP would vary as a function of the timing between pre- and postsynaptic events.

Here, we investigated the timing dependency of long-term synaptic plasticity in the hippocampal CA1 region using field recordings and extracellular stimulation of pre- and postsynaptic components of CA1 neurons by timed activation of Schaffer collaterals (SC) and CA1 axons in the alveus, respectively. Furthermore, we tested some of the molecular mechanisms mediating STDP expression and maintenance using pharmacological approaches. Finally, we examined the participation of STDP in late associativity, STC, in CA1 neurons.

Results

Coincidental Pre- and Postsynaptic Stimulation Induces Input-Specific Population STDP. Most systematic investigations of STDP in acute rat hippocampal slices were conducted using juvenile animals ($P < 28$) (14, 15, 17–19). Using whole-cell patch-clamp recordings in acute slices, some groups have shown that while pairing of SC stimulation with single postsynaptic spikes is sufficient to induce potentiation in juvenile animals, pairing of presynaptic stimulation with bursts of postsynaptic action potential is needed for the induction of potentiation in adult rats (14, 16, 17, 20). Therefore, we first investigated whether pairing of SC and alveus layer axon stimulation was sufficient to induce changes in synaptic strength in CA3–CA1 synapses in young adult [postnatal day (P) 35–49] rat acute hippocampal slices (Fig. 1 *A* and *B*). The stimulation of alveus layer axons is known to induce antidromic action potentials in CA1 pyramidal neurons (21). A significant potentiation was observed immediately after 20 pairings of simultaneous stimulations of synaptic input S1 in the stratum radiatum (s.r.) and alveus layer axons of CA1 pyramidal neurons (S0; relative timing interval between S0 and S1 stimulations $\Delta t = 0$ ms) at 1 Hz [Fig. 1*C*, red circles; $n = 7$; at +30 min, normalized field excitatory postsynaptic potential (fEPSP) = 139.5 ± 6.86% of baseline; +30 min vs. −15 min, Wilcox test, $P = 0.02$]. The synaptic potentiation stabilized within 30 min and lasted for 4 h (Fig. 1*C*; at +240 min, normalized fEPSP = 138.4 ± 9.15%; +240 min vs. −15 min, Wilcox test, $P = 0.02$; at +240 min, S1 vs. S2, Mann–Whitney *U* test, $P = 0.002$). The potentiation was input-specific as no significant changes in fEPSPs were observed in the unpaired control input S2 (Fig. 1*C*, blue circles; at +240 min, normalized fEPSP = 100.8 ± 4.85%; +240 min vs. −15 min, Wilcox test, $P = 0.58$). In contrast, lasting potentiation in input S1 was not observed with alveus stimulation alone (20 repeats at 1 Hz; see *SI Appendix*, Fig. S1*A*) or with SC stimulation alone (20 repeats, 1 Hz; see *SI Appendix*, Fig. S1*B*). Although 20 repeats of presynaptic stimulation alone resulted in a slight increase in fEPSPs, this potentiation was brief and much lower than that observed in response to pairing of pre- and postsynaptic stimulations. Furthermore, no change in synaptic transmission was observed when simultaneous s.r. and stratum oriens stimulations were given (*SI Appendix*, Fig. S1*D*). This suggests that the coupling of pre- and postsynaptic activities was required for persistent potentiation, as depicted in Fig. 1*C*.

Furthermore, as a proof of concept, we repeated the experiments with whole-cell patch-clamp recordings. We measured single-cell EPSPs in CA1 pyramidal neurons evoked by stimulation of the s.r. and applied the same population STDP (pSTDP) induction protocol to induce synaptic plasticity. Similar to the field recordings, repeated pairing of extracellular s.r. and alveus stimulations ($\Delta t = 0$ ms) led to a significant increase in EPSPs in single CA1 pyramidal neurons (Fig. 1*D*, red circles; $n = 7$; at +17.5 min, normalized EPSP = 249.4 ± 66.88%; +17.5 min vs. −1.5 min, Wilcox test, $P = 0.03$). In addition, repeated stimulation of the s.r. or alveus alone did not lead to significant changes in single-cell EPSPs in CA1 neurons (Fig. 1*E*, red circles; $n = 7$; at +17.5 min, normalized EPSP = 126.8 ± 27.05%; +17.5 min vs. −1.5 min, Wilcox test, $P = 1.00$; Fig. 1*F*, red circles; $n = 5$; at +17.5 min, normalized EPSP = 101.5 ± 8.46%; +17.5 min vs. −1.5 min, Wilcox test, $P = 0.63$).

In summary, pairing of presynaptic SC stimulation with alveus stimulation at a low frequency (1 Hz) was sufficient to induce long-lasting potentiation of synaptic transmission of SC-CA1 synapses. This change in synaptic strength will be referred to as pSTDP henceforth.

Strength and Persistence of Synaptic Modification Are Dependent on the Relative Timing and Order of Pre- and Postsynaptic Activities. The relative timing between SC stimulation (S1) and alveus stimulation (S0) was systematically varied to investigate the effect of spike timing on the endurance of synaptic modification. Forward pairing of pre- and postsynaptic stimulations at positive timing intervals ($\Delta t = 10$ to 40 ms; Fig. 2) led to potentiations of various persistence. When presynaptic stimulation (S1) of SC preceded the alveus stimulation (S0) by 10 to 20 ms ($\Delta t = 10$ and 20 ms; Fig. 2 *A* and *C*), a lasting fEPSP potentiation was observed in S1 for 4 h (Fig. 2*A*, red circles; $n = 8$; S1: at +240 min, normalized fEPSP = 130.2 ± 9.39%; +240 min vs. +15 min, Wilcox test, $P = 0.02$; at +240 min, S1 vs. S2, Mann–Whitney *U* test, $P = 0.007$; Fig. 2*C*, red circles; $n = 11$; S1: at +240 min, normalized fEPSP = 116.1 ± 6.22%; +240 min vs. +15 min, Wilcox test, $P = 0.03$; at +240 min, S1 vs. S2, Mann–Whitney *U* test, $P = 0.02$). The potentiation observed with $\Delta t = 10$- to 20-ms paired stimulations appeared to be lower in magnitude than that elicited by simultaneous pre- and postsynaptic stimulations, although the maintenance of the potentiation in all three experimental paradigms was equal. The control input S2 did not show any significant changes in both sets of experiments (Fig. 2*A*, blue circles; at +240 min, normalized fEPSP = 97.77 ± 6.05%; +240 min vs. −15 min, Wilcox test, $P = 0.55$; Fig. 2*C*, blue circles; at +240 min, normalized fEPSP = 97.02 ± 3.49%; +240 min vs. −15 min, Wilcox test, $P = 0.37$).

When the synaptic input S1 was stimulated 30 ms before the alveus ($\Delta t = 30$ ms), a small but significant potentiation was observed in the paired input S1 (Fig. 2*E*, red circles). The potentiation was statistically significant until 140 min ($n = 10$; at +140 min, normalized fEPSP = 113.0 ± 4.26%; +140 min vs. −15 min, Wilcox test, $P = 0.03$; at +140 min, S1 vs. S2, Mann–Whitney *U* test, $P = 0.01$), after which the fEPSP gradually returned to baseline (at 240 min, normalized fEPSP = 101.0 ± 9.49%; +240 min vs. −15 min, Wilcox test, $P = 0.92$; at +240 min, S1 vs. S2, Mann–Whitney *U* test, $P = 0.48$). Similarly, pairing of presynaptic (S1) and postsynaptic (S0) stimulations with a relative timing interval of $\Delta t = 40$ ms resulted in a slight potentiation in the paired input S1 (Fig. 2*G*, red circles) that was statistically significant until 70 min after pairing and eventually decayed to baseline ($n = 11$; at +70 min, normalized fEPSP = 112.2 ± 5.72%; +70 min vs. −15 min, Wilcox test, $P = 0.03$; at +70 min, S1 vs. S2, Mann–Whitney *U* test, $P = 0.04$). No significant changes were observed in the control input S2 in either sets of experiments (Fig. 2 *E* and *G*, blue circles; Fig. 2*E*, S2: at +240 min, normalized fEPSP = 96.47 ± 4.17%; +240 min vs. −15 min, Wilcox test, $P = 0.97$; Fig. 2*G*, S2: at +240 min,

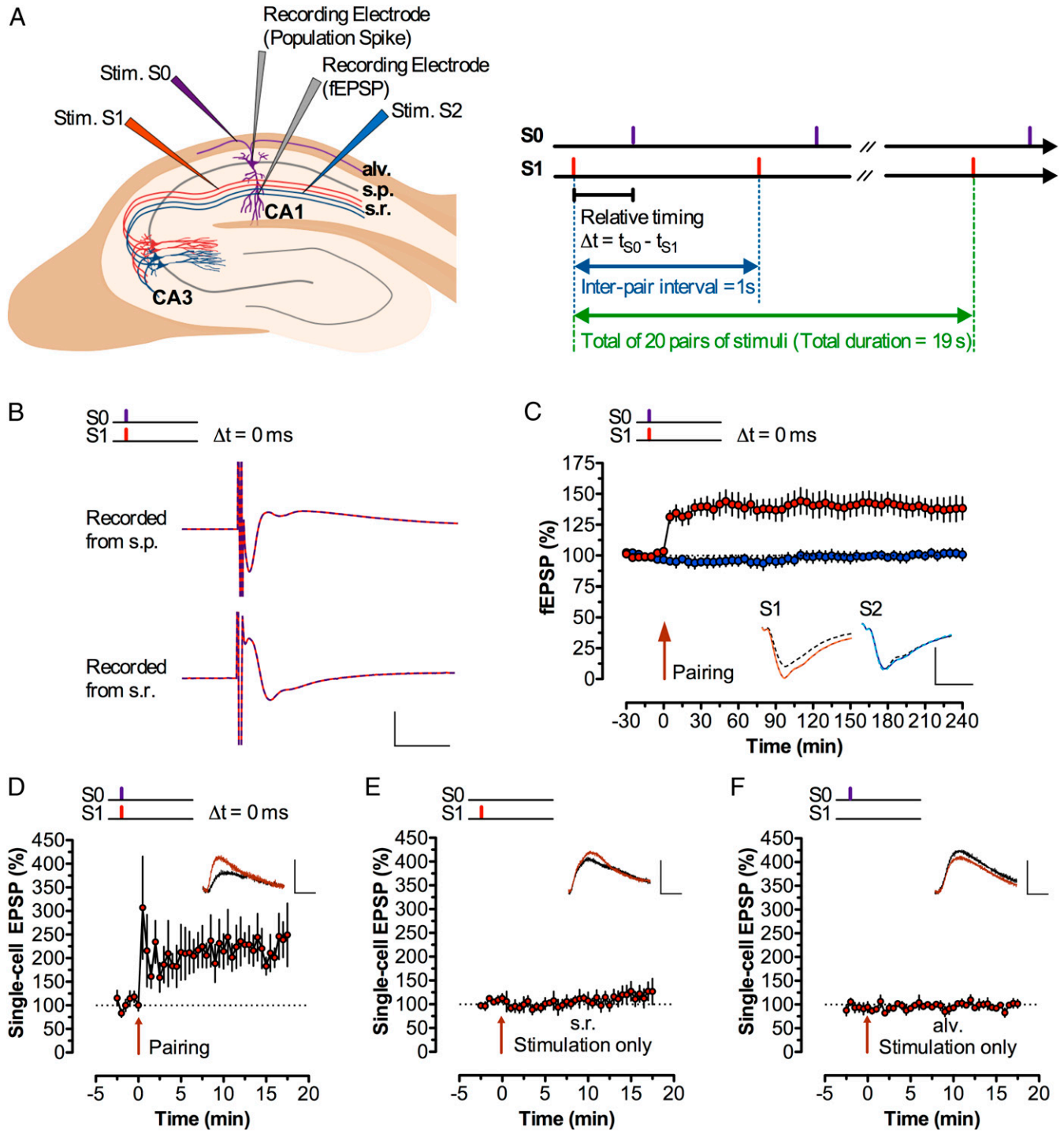

Fig. 1. Pairing-dependent induction of persistent potentiation in hippocampal CA1 pyramidal neurons. (*A*) A schematic diagram of electrode locations and stimulation protocol in electrophysiology experiments is depicted. The two gray inverted triangles represent recording electrodes placed in the stratum pyramidale (s.p.) and s.r. of acute adult rat hippocampal slices. Red and blue triangles represent two stimulating electrodes (Stim. S1 and Stim. S2) that were placed in the s.r. to stimulate two independent SC pathways, and the purple triangle represents a stimulating electrode (Stim. S0) located in the alveus (alv.) layer to elicit antidromic action potentials in CA1 pyramidal neurons. Purple and red bars represent the timings at which postsynaptic and presynaptic stimulations were delivered, respectively. Relative timing $\Delta t = t_0 - t_1$, where t_0 and t_1 are the time points at which stimulus S0 (postsynaptic component) and S1 (presynaptic component) were initiated. (*B*) Analog traces representing field potentials that were typically recorded from the s.p. and s.r. in response to simultaneous pairing of alv. (Stim. S0) and s.c. (Stim. S1) stimulation. (*C*) Simultaneous extracellular stimulation (arrow) of the presynaptic input S1 and the alv. layer (S0) (20 pairings, 1 Hz) induced a persistent pathway-specific increase in synaptic responses of input S1 (red circles) that lasted 4 h. Unpaired input S2 (blue circles) remained stable ($n = 7$). (*D*) Single-cell EPSPs displayed significant potentiation after pairing of simultaneous extracellular s.r. and alv. stimulations ($n = 7$). (*E*) Twenty repeats of s.r. stimulation alone did not lead to any changes in single-cell EPSPs ($n = 7$). (*F*) Repeated alv. stimulation alone did not lead to changes in single-cell EPSPs ($n = 5$). All data are shown as mean ± SEM. In *C*, analog traces show representative fEPSPs at 15 min before (S1 and S2: black dashed lines), 30 min after (S1: orange dashed line; S2: turquoise dashed line), and 240 min after (S1: red solid line; S2: blue solid line) the induction of pSTDP. In *D–F*, analog traces show representative single-cell EPSPs before (black lines) and after (red line) pairing or the delivery of other stimulation protocols. (Scale bars for analog traces in *B*: 5 mV/10 ms, *C*: 3 mV/5 ms, *D–F*: 4 mV/10 ms.)

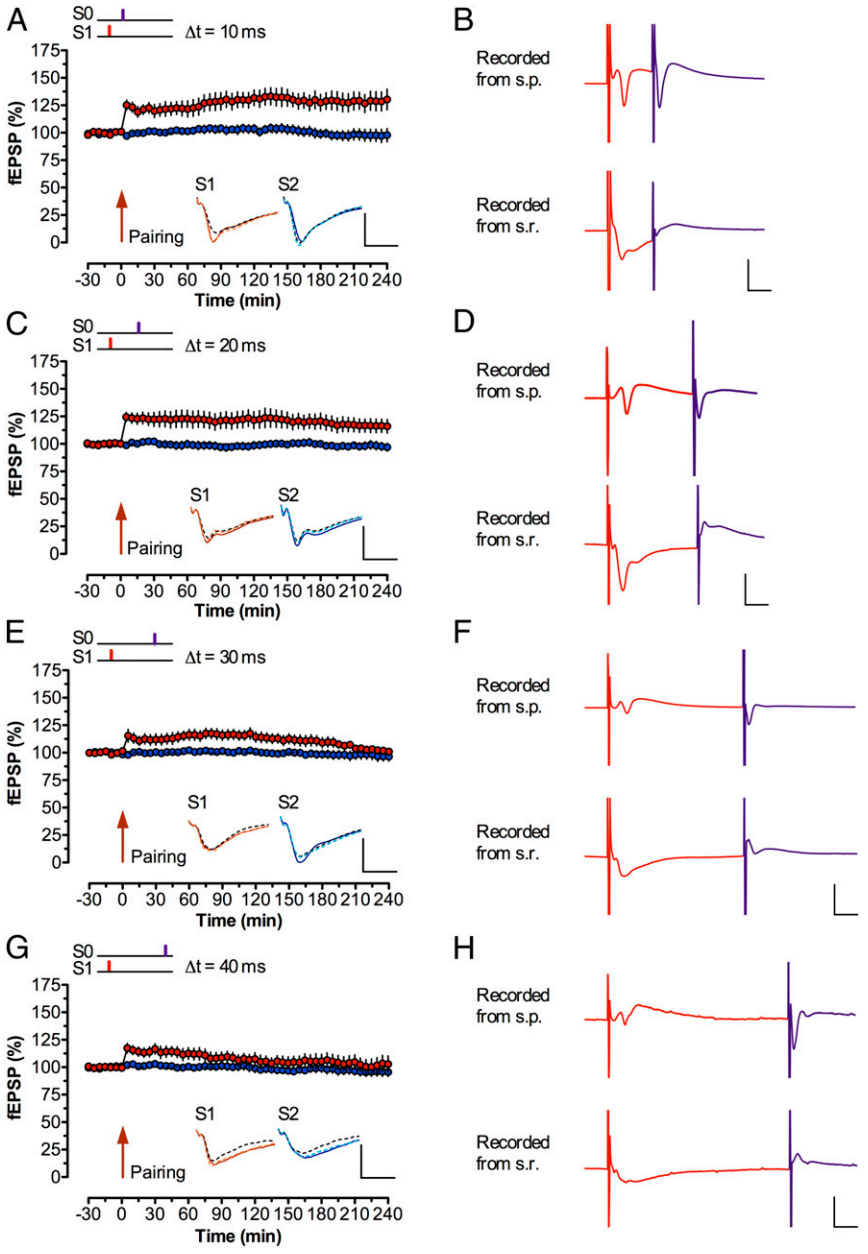

Fig. 2. Potentiation of various persistence ensues when presynaptic pathway activity precedes postsynaptic pathway activity within a time window of 40 ms in the hippocampal area CA1. Normalized fEPSP plasticity induced by pairing protocols with different time intervals between extracellular stimulation of SC pathway S1 (red bar) and subsequent alveus (alv.) stimulation S0 (purple bar). (*A*) Persistent potentiation of 4 h was observed in the synaptic input S1 (red circles) after pairing of s.c. stimulation S1 (red bar) with subsequent alv. stimulation S0 (purple bar) with a 10-ms time difference ($n = 8$). (*B*) Representative analog traces of extracellular recordings at the stratum pyramidal (s.p.) and s.r. layers during pairing of s.c. stimulation and subsequent alv. stimulation at a relative timing of 10 ms. Traces in red represent those elicited by stimulation of presynaptic pathway S1 and traces in purple represent those evoked by alv. stimulation S0. (*C*) Pairing (arrow) of s.c. S1 (red bar) and alv. S0 (purple bar) stimulations at a relative timing interval of 20 ms resulted in a statistically significant potentiation in pathway S1 (red circles) that lasted throughout the recording ($n = 11$). (*D*) Representative analog traces of pairing at a relative timing of 20 ms are shown. (*E*) Following pairing (arrow) of s.c. stimulation S1 (red bar) and alv. stimulation S0 (purple bar) with a relative timing of 30 ms, pathway S1 (red circles) displayed a potentiation that was statistically significant until 140 min ($n = 10$). (*F*) Representative analog traces of pairing at a relative timing of 30 ms are depicted. (*G*) Pairing (arrow) of s.c. stimulation S1 (red bar) and alv. stimulation S0 (purple bar) with a relative timing of 40 ms resulted in a transient potentiation that decayed to baseline within 70 min in the paired input S1 (red circles; $n = 11$). (*H*) Representative analog traces of pairing at a relative timing of 40 ms are shown. The control input S2 (blue circles) showed no observable change in fEPSPs in all experiment series *A*, *C*, *E*, and *G*. All data show mean ± SEM. Analog traces show representative fEPSPs at 15 min before (S1 and S2: black dashed line), 30 min after (S1: orange dashed line; S2: turquoise dashed line), and 240 min after (S1: red solid line; S2: blue solid line) the induction of pSTDP. (Scale bars for analog traces in *A*, *C*, *E*, and *G*: 3 mV/5 ms; in *B*, *D*, *F*, and *H*: 5 mV/5 ms.)

normalized fEPSP = 95.67 ± 4.10%; +240 min vs. −15 min, Wilcox test, $P = 0.28$).

In contrast, post-pre backward pairing had a smaller potentiation window and seemingly greater variation in maintenance (Fig. 3). When alveus stimulation (S0) was followed by presynaptic stimulation (S1) by 10 ms ($\Delta t = -10$ ms), an input-specific potentiation that lasted for 4 h was observed in the paired input S1 (Fig. 3*A*, red circles; $n = 7$; at +240 min, normalized fEPSP = 132.6 ± 9.26%; +240 min vs. −15 min, Wilcox test, $P = 0.02$; at +240 min, S1 vs. S2, Mann–Whitney *U* test, $P = 0.02$). No discernable changes were observed in the unpaired input S2 (Fig. 3*A*, blue circles; at +240 min, normalized fEPSP = 95.52 ± 6.74%; +240 min vs. −15 min, Wilcox test, $P = 0.69$). Stimulating the alveus layer (S0) 20 ms before stimulating the presynaptic pathway S1 ($\Delta t = -20$ ms) resulted in a short-term potentiation in S1 that was statistically significant until 20 min (Fig. 3*C*, red circles; $n = 7$; at +20 min, normalized fEPSP = 110.6 ± 3.72%; +20 min vs. −15 min, Wilcox test, $P = 0.03$; at +20 min, S1 vs. S2, Mann–Whitney *U* test, $P = 0.04$). Afterward, synaptic efficacy in S1 gradually decreased. The depression stabilized and became statistically significant from 175 min onward (at +175 min, normalized fEPSP = 87.05 ± 3.52%; +175 min vs. −15 min, Wilcox test, $P = 0.03$; at +175 min, S1 vs. S2, Mann–Whitney *U* test, $P = 0.02$). Throughout the recording period, control input S2 remained stable (blue circles; at +240 min, normalized fEPSP = 99.48 ± 3.59%; +240 min vs. −15 min, Wilcox test, $P = 1.00$). Following repeated pairing of alveus stimulation at 30 ms before s.r. stimulation ($\Delta t = -30$ ms), no significant changes in synaptic efficacy were observed in both the paired input S1 and the control input S2 throughout the recording session (Fig. 3*E*; $n = 8$; S1, red circles: at +240 min, normalized fEPSP = 99.31 ± 5.03%; +240 min vs. −15 min, Wilcox test, $P = 0.95$; S2, blue circles: at +240 min, normalized fEPSP = 100.8 ± 4.72%; +240 min vs. −15 min, Wilcox test, $P = 0.84$; at +240 min, S1 vs. S2, Mann–Whitney *U* test, $P = 0.88$).

The results from Figs. 2 and 3 are summarized in Fig. 4. In brief, we observed an asymmetric pSTDP curve that changed

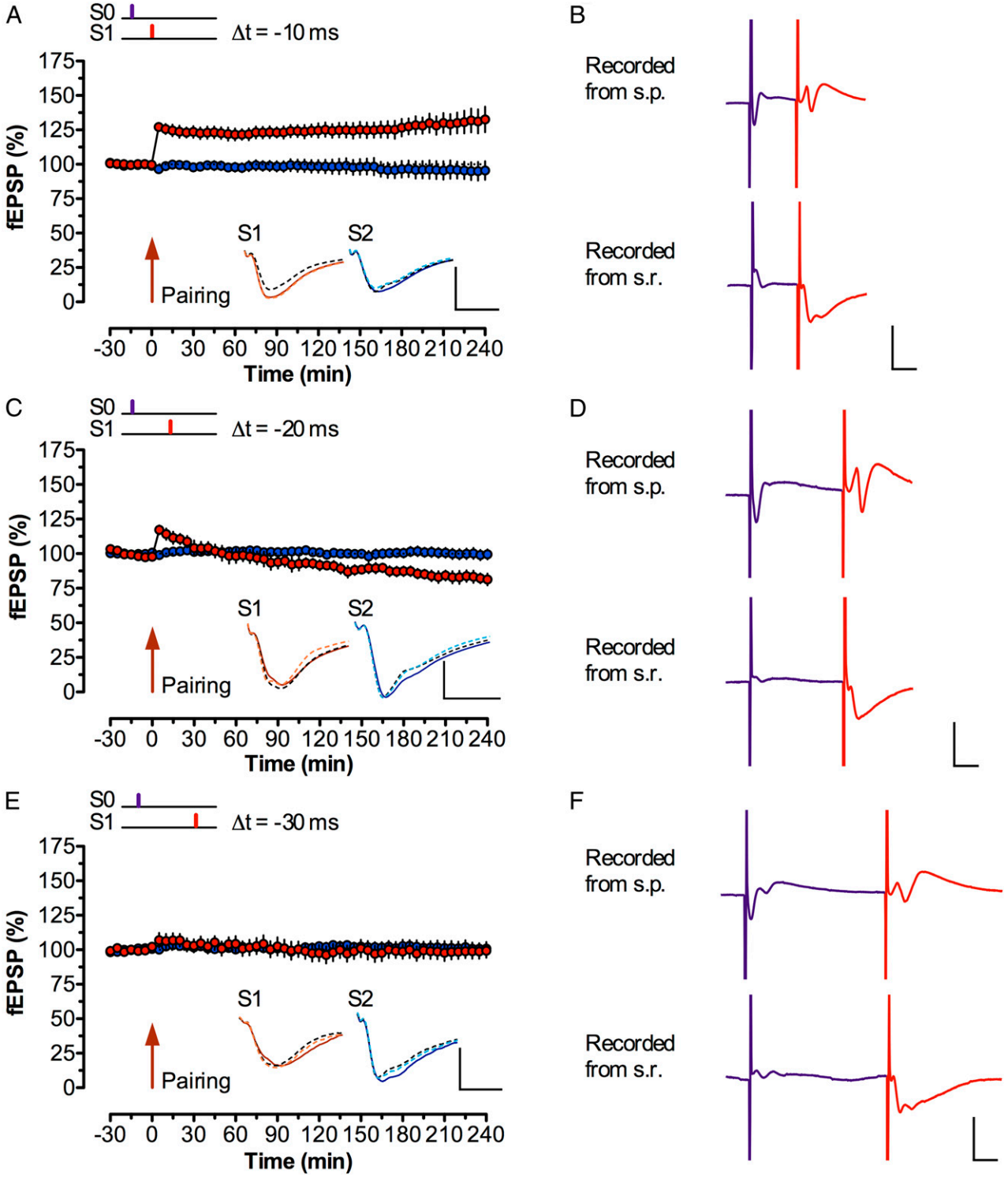

Fig. 3. Bidirectional synaptic plasticity of SC-CA1 synapses when presynaptic activity follows postsynaptic activity within a timing window of up to 30 ms. fEPSP plasticity was induced by different pairing protocols with time lags from 0 to 30 ms between alveus (alv.) stimulation S0 (purple bar) and subsequent extracellular stimulation of SC pathway S1 (red bar). (*A*) Persistent potentiation in S1 (red circles) resulted from repeated pairing (arrow) of alv. stimulation (S0) and subsequent s.c. stimulation (S1) with a relative time lag of −10 ms. Potentiation in S1 was statistically significant until the end of the recording ($n = 7$). (*B*) Representative analog traces of extracellular recordings at the stratum pyramidal (s.p.) and s.r. layers during pairing of presynaptic stimulation (red) and subsequent postsynaptic stimulation (purple) at a relative timing of −10 ms are shown. (*C*) When alv. stimulation S0 preceded s.c. stimulation S1 by 20 ms (arrow), a transient potentiation was observed in input S1 (red circles). fEPSP slope in S1 gradually decreased after pairing and stabilized into a statistically significant depression from 175 min onward ($n = 7$). (*D*) Representative analog traces of pairing at a relative timing of −20 ms are shown. (*E*) Pairing (arrow) of s.c. stimulation (S1) and alv. stimulation (S0) at a relative timing interval of −30 ms had no effect on synaptic transmission in both the paired pathway S1 (red circles; $n = 8$). (*F*) Representative analog traces of pairing at a relative timing of −30 ms are shown. The control input S2 (blue circles) showed no observable change in fEPSPs in all experiment series *A*, *C*, and *E*. All data show mean ± SEM. Analog traces show representative fEPSPs at 15 min before (S1 and S2: black dashed line), 30 min after (S1: orange dashed line; S2: turquoise dashed line), and 240 min after (S1: red solid line; S2: blue solid line) the induction of pSTDP. (Scale bars for analog traces in *A*, *C*, *E*, and *G*: 3 mV/5 ms; in *B*, *D*, *F*, and *H*: 5 mV/5 ms.)

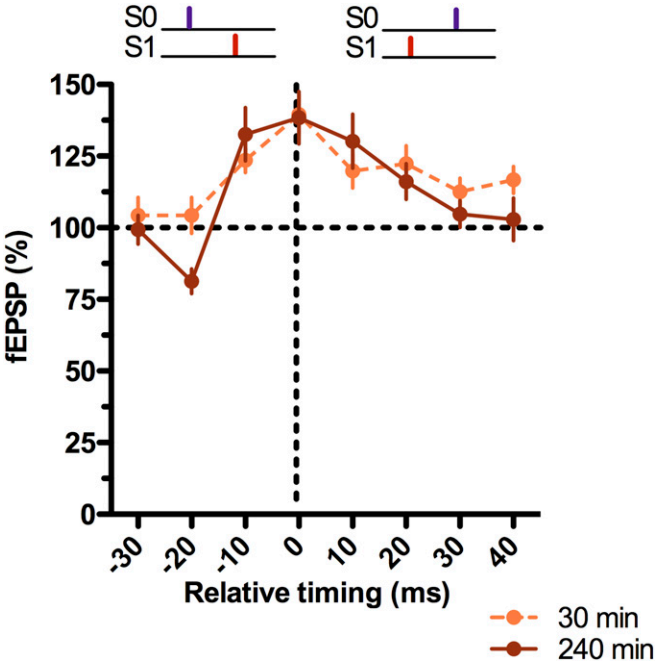

Fig. 4. Inverted-U-curve-like dependency of fEPSP potentiation on the timing of pre- and postsynaptic activity. Changes in synaptic transmission resulted from pairing of SC stimulation (red bar) and alveus stimulation (purple bar) are summarized in this graph. The relative increase of fEPSP slopes at 30 min (orange circles) or 240 min (red circles) after pSTDP induction are plotted against relative timings of pre- and postsynaptic stimulations. Magnitude and persistence of synaptic change differ as a function of the relative pairing timing. All data show mean ± SEM.

over time: immediately after pSTDP induction, successive pairing of presynaptic stimulation and postsynaptic stimulation within 40 ms ($\Delta t \leq 40$ ms) led to fEPSP potentiation, but when presynaptic stimulation followed the postsynaptic one, instantaneous potentiation was only observed when the two events were separated by no more than 20 ms ($\Delta t \geq -20$ ms). However, 4 h after pSTDP induction, the endurance of pSTDP differed such that the efficient pairing time window narrowed down to -10 ms $\leq \Delta t \leq 20$ ms. Notably, a depression was observed at $\Delta t = -20$ ms, while no change in synaptic transmission was observed beyond $\Delta t = 30$ ms and $\Delta t = -30$ ms.

Interestingly, when we doubled the number of repeats (from 20 to 40 pairs), the pairing of presynaptic (S1) and postsynaptic (S0) stimulations at a relative timing interval of $\Delta t = 40$ ms resulted in a slight, transient potentiation (*SI Appendix*, Fig. S2*A*). This potentiation was similar in magnitude but slightly more persistent than that observed with 20 pairing repeats (Fig. 2*G*). However, 60 pairings at $\Delta t = 40$ ms did not lead to any observable changes in synaptic transmission in both the test input S1 and the control input S2 (*SI Appendix*, Fig. S2*B*). These results suggest that the number of pairing repeats influences the pSTDP curve as well.

pSTDP Requires CaMKII Signaling but Not Extracellular BDNF. We next examined some of the possible molecular mediators of pSTDP. First, TrkB-Fc (1 $\mu g \cdot mL^{-1}$), which chelates extracellular BDNF, was bath-applied to the hippocampal slices 30 min before and after pSTDP induction ($\Delta t = 0$ ms; Fig. 5*A*). Perfusion of TrkB-Fc had no discernible effects on the expression and the maintenance of pSTDP; pairing at 0 ms resulted in a potentiation that lasted until the end of the 4-h recordings (Fig. 5*A*, red circles; $n = 7$; at +240 min, normalized fEPSP = 139.8 ± 11.11%; +240 min vs. −30 min, Wilcox test, $P = 0.03$; at +240 min, S1 vs. S2, Mann–Whitney *U* test, $P = 0.03$). Application of the soluble ligand did not affect basal transmission of the control input S2 (blue circles; at +240 min, normalized fEPSP = 99.11 ± 6.05%; +240 min vs. −30 min, Wilcox test, $P = 0.94$). These experiments suggest that pSTDP induced by our protocol was not dependent on extracellular BDNF.

In contrast, bath application of KN-93, which selectively inhibits CaMKII at the concentration used (1 μM), prevented pSTDP induction by repeated pairing of alveus (S0) and s.r. (S1) activation ($\Delta t = 0$ ms). In the presence of KN-93, pairing led to a slight facilitation of fEPSP, which returned to baseline within 40 min (Fig. 5*B*, red circles; $n = 8$; at +35 min, normalized fEPSP = 107.8 ± 2.86%; +35 min vs. −30 min, Wilcox test, $P = 0.04$; at +35 min, S1 vs. S2, Mann–Whitney *U* test, $P = 0.01$). Field EPSP in S1 at the end of the recording was not significantly different from the baseline values (at +240 min, normalized fEPSP = 101.8 ± 5.74%; +240 min vs. −30 min, Wilcox test, $P = 0.55$; at +240 min, S1 vs. S2, Mann–Whitney *U* test, $P = 0.33$). As a control, KN-92 (an inactive analog of KN-93) was also bath-applied to slices at 1 μM. Induction of pSTDP ($\Delta t = 0$ ms) in the presence of KN-92 resulted in persistent potentiation that lasted 4 h (Fig. 5*C*, red circles; $n = 7$; at +240 min, normalized fEPSP = 138.0 ± 11.97%; +240 min vs. −30 min, Wilcox test, $P = 0.03$; at +240 min, S1 vs. S2, Mann–Whitney *U* test, $P = 0.02$), similar to that observed in control conditions. In both Fig. 5 *B* and *C*, control input S2 was not affected by the drug application and pSTDP induction in S1, and fEPSP in S2 remained at baseline levels throughout the experiment (Fig. 5*B*, blue circles; at +240 min, normalized fEPSP = 95.69 ± 4.69%; +240 min vs. −30 min, Wilcox test, $P = 0.31$; Fig. 5*C*, blue circles; at +240 min, normalized fEPSP = 103.9 ± 5.01%; +240 min vs. −30 min, Wilcox test, $P = 0.47$). The above experiments indicate that CaMKII signaling is likely required for pSTDP induction.

Additionally, bath application of AP5 (50 μM), an NMDA receptor antagonist, during the induction of pSTDP completely blocked pSTDP expression (*SI Appendix*, Fig. S3*A*), suggesting the requirement of NMDA receptors for pSTDP induction.

pSTDP Engages in Selective Forms of Long-Term Associativity: Promoting STC but Not Cross-Tagging. In addition to the need for CaMKII and NMDA receptors for pSTDP expression, we observed that pSTDP also required protein synthesis for prolonged maintenance (*SI Appendix*, Fig. S3 *B* and *C*). Bath application of protein synthesis inhibitors emetine (20 μM) or anisomycin (25 μM) during pSTDP induction did not impair the initial expression of pSTDP but impeded its maintenance. As pSTDP required de novo translation for the stabilization of synaptic enhancement, we investigated whether the implicated up-regulation of PRPs triggered by pSTDP induction could influence the modification of neighboring activated synapses, as implied in the STC hypothesis (7, 9). To this end, an experimental procedure akin to the "strong before weak" paradigm (8) was employed. After a stable baseline was obtained in the inputs S1 and S2, pSTDP was induced in S1 (Fig. 6*A*, red circles) by pairing of alveus (S0) and s.r. (S1) stimulations at a relative timing interval of $\Delta t = 0$ ms. One hour thereafter, early LTP (which usually decays to baseline within 1 to 3 h; see *SI Appendix*, Fig. S4*A*) was induced in presynaptic input S2 (Fig. 6*A*, blue circles) by a "weak" tetanization (WTET). pSTDP induction in S1 resulted in a statistically significant potentiation that lasted for 4 h (Fig. 6*A*, red circles; $n = 11$; at +240 min, normalized fEPSP = 147.1 ± 10.84%; +240 min vs. −15 min, Wilcox test, $P = 0.001$), while pairing had no observable effects on basal transmission in S2 (blue circles; at +60 min, normalized fEPSP = 104.6 ± 2.67%; +60 min vs. −15 min, Wilcox test, $P = 0.24$). After the induction of WTET, S2 expressed an immediate increase in fEPSP that was statistically significant until the end of the recording (at +240 min, normalized fEPSP = 140.2 ± 15.66%;

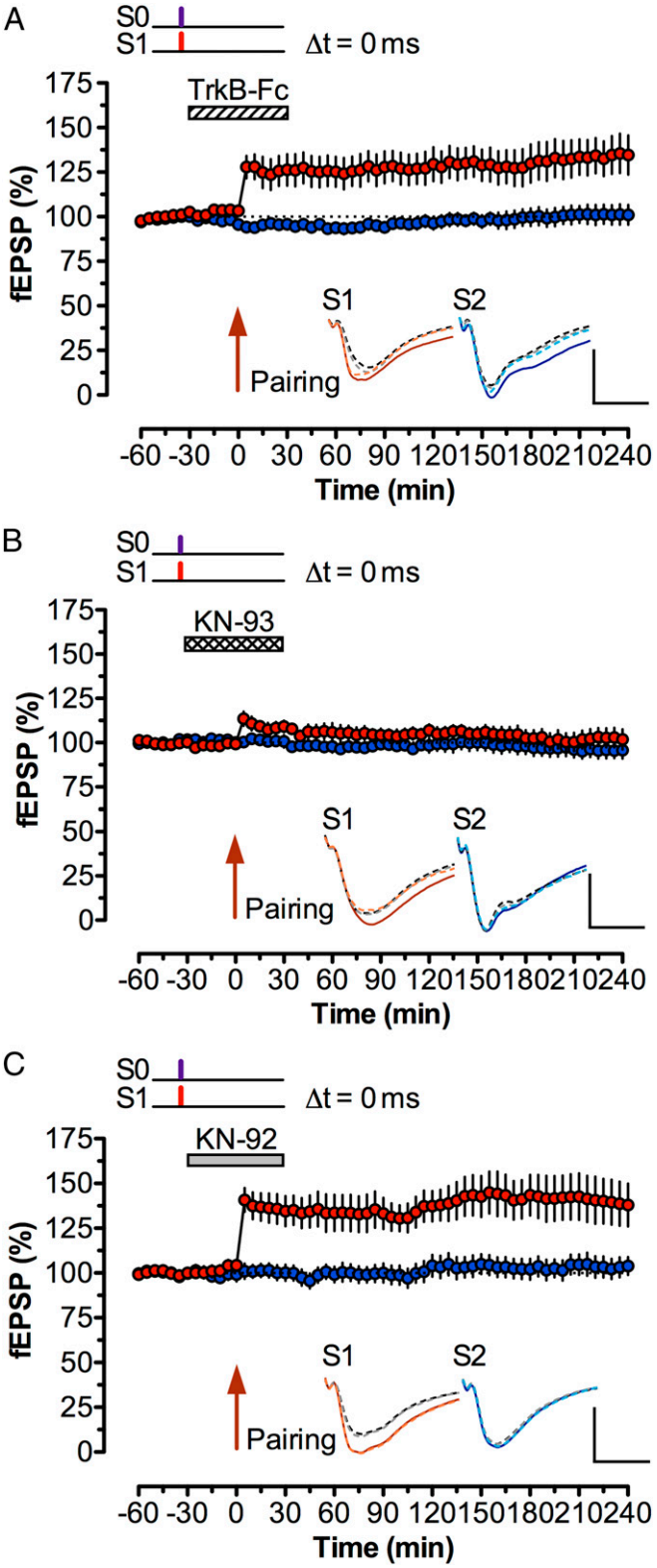

Fig. 5. pSTDP is dependent on CaMKII signaling but not BDNF/TrkB-Fc signaling. (*A*) Bath application of TrkB-Fc (1 μg·mL^{-1}; striped box) during simultaneous stimulations (arrow) of presynaptic input S1 (red circles) and alveus (S0) had no effect on the induction of pSTDP (n = 7). (*B*) pSTDP induction (arrow) was blocked by the bath application of KN-93 (1 μM; cross-hatched box), a CaMKII inhibitor. fEPSP in paired input S1 (red circles) showed a slight potentiation that returned to baseline within 40 min, while control input S2 (blue circles) remained stable (n = 8). (*C*) Bath application of KN-92 (1 μM; solid box), an inactive analog of KN-93, had no significant effects on the induction of pSTDP. All data show mean ± SEM. Analog traces show representative field EPSPs at 15 min before drug application (S1 and S2: black dashed lines), 15 min after drug application (S1 and S2: gray dashed lines), 30 min after (S1: orange dashed line; S2: turquoise dashed line), and 240 min after (S1: red solid line; S2: blue solid line) the induction of pSTDP. (Scale bars for analog traces in *A*–*C*: 3 mV/5 ms.)

+240 min vs. −15 min, Wilcox test, P = 0.0068). Similarly, we tested whether a "strong" pSTDP induction (Δt = 0 ms) could reinforce a "weak," short-lasting pSTDP (Δt = 40 ms). As expected, pSTDP induction by repeated simultaneous presynaptic (S1) and postsynaptic (S0) stimulations (Δt = 0 ms) led to an immediate potentiation in S1 that lasted for 4 h (Fig. 6*B*, red circles; n = 6; at +240 min, normalized fEPSP = 137.7 ± 7.87%; +240 min vs. −15 min, Wilcox test, P = 0.03). One hour after pSTDP induction in S1, stimulation of another independent presynaptic input S2 was repeatedly paired with alveus (S0) stimulation at a relative timing interval of Δt = 40 ms. Although it usually led to short-term potentiation only (Fig. 2*G*), pairing at Δt = 40 ms led to a statistically significant potentiation that lasted for at least 3 h when it followed a "strong" pSTDP induction (Δt = 0 ms) in a separate pathway (Fig. 6*B*, blue circles; n = 6; at +240 min, normalized fEPSP = 132.2 ± 10.39%; +240 min vs. −15 min, Wilcox test, P = 0.03). Together, these results imply that pSTDP induction triggers the synthesis of PRPs in amounts sufficient to be shared across multiple synapses potentiated by different events.

Subsequently, we examined whether the pSTDP-induced PRPs are process-specific, that is, whether these PRPs can only be captured and utilized by potentiated synapses or whether some of those PRPs can also support the maintenance of LTD. Hence, we explored the possible interactions between pSTDP and LTD using the "cross-tagging" paradigm (10). pSTDP was induced in the presynaptic pathway S1 by the pairing of simultaneous S0 and S1 stimulations (Fig. 6*C*, red circles); 30 min after pSTDP induction, transient early LTD was induced in an independent pathway S2 by "weak" low-frequency stimulation (WLFS) (Fig. 6*C*, blue circles). Early LTD induced by WLFS typically returns to baseline levels within 2 h (*SI Appendix*, Fig. S4*B*). If early LTD could cross-capture the pSTDP-induced PRPs, it would be transformed into a long-lasting late LTD. In Fig. 6*C*, induction of pSTDP led to a statistically significant potentiation in S1 that lasted for 4 h (Fig. 6*C*, red circles; n = 7; at +240 min, normalized fEPSP = 142.0 ± 7.75%; +240 min vs. −15 min, Wilcox test, P = 0.02), while WLFS in S2 only led to a transient depression that was statistically significant until 210 min (Fig. 6*C*, blue circles; at +210 min, normalized fEPSP = 93.21 ± 3.34%; +210 min vs. −15 min, Wilcox test, P = 0.05). This suggests that pSTDP could not strengthen early LTD into prolonged LTD. In contrast, cross-tagging was observed when late LTP induced by "strong" tetanization (STET) supported the reinforcement of early LTD into late LTD in a separate pathway (Fig. 6*D*). STET induced LTP that lasted for 4 h in S1 (Fig. 6*D*, red circles; n = 7; at +240 min, normalized fEPSP = 160.3 ± 12.55%; +240 min vs. −15 min, Wilcox test, P = 0.02). Thirty minutes after STET, WLFS was applied to an independent pathway S2 (blue circles). This led to a significant decrease in fEPSP that was stable until the end of the recording (at +240 min, normalized fEPSP = 63.91 ± 3.76%; +240 min vs. −15 min, Wilcox test, P = 0.02).

To address the possibility that pSTDP induction increased the excitability of the neuronal population and hence the threshold for LTD induction, we reversed the order of pSTDP and early LTD induction. Nevertheless, we did not observe positive late association of LTD and pSTDP (Fig. 6*E*). When early LTD was induced in the synaptic pathway S1, a significant decrease in fEPSP was observed immediately after WLFS, yet the fEPSP gradually reverted to baseline. The depression was statistically

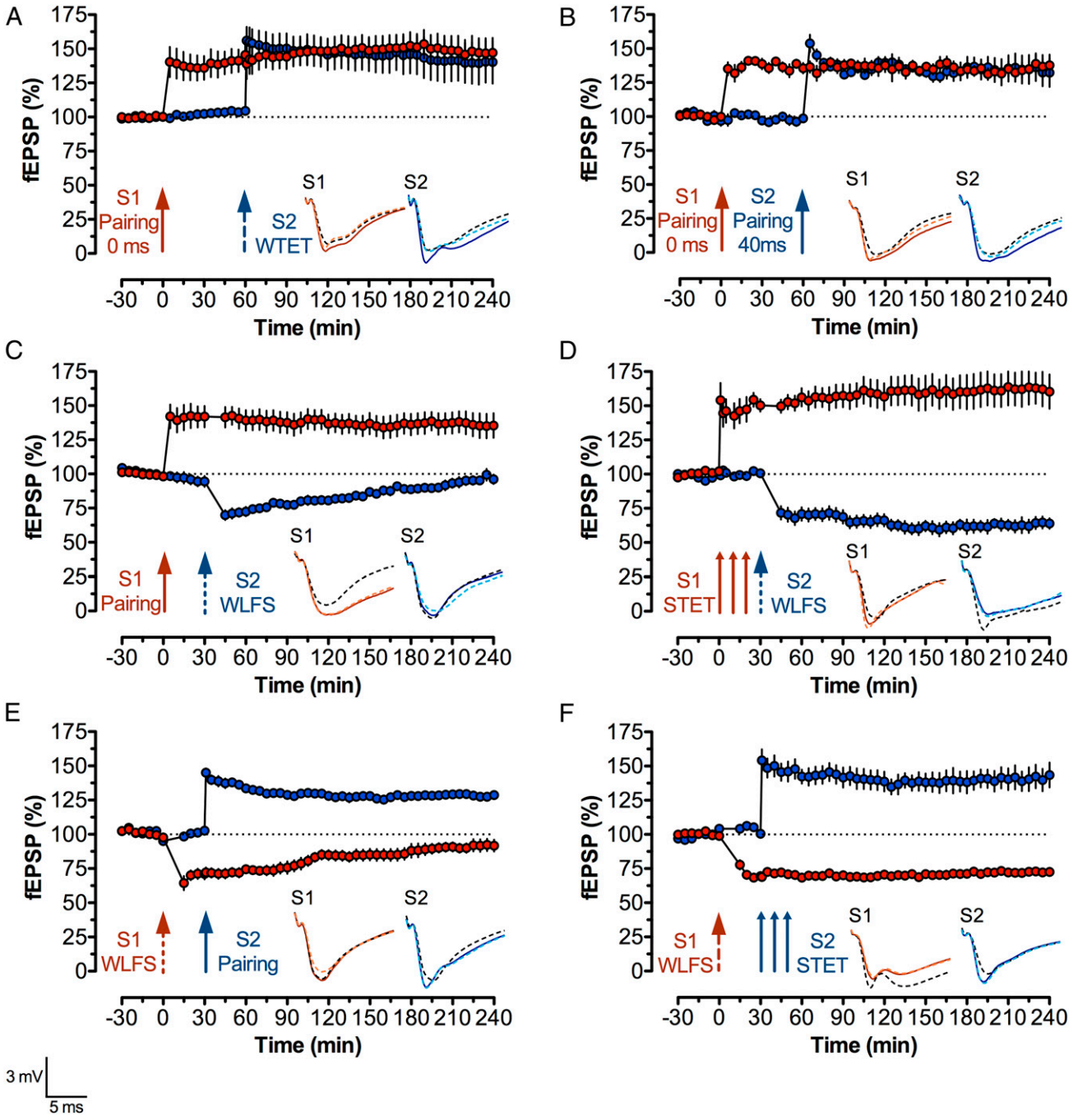

Fig. 6. pSTDP reinforces early LTP into late LTP in a neighboring pathway but does not support the maintenance of LTD. (*A*) Pairing (solid arrow) of simultaneous pre- (S1) and postsynaptic (S0) pathway stimulations resulted in a statistically significant potentiation in the paired input S1 (red circles) without affecting the unpaired input S2 (blue circles). Induction of early LTP (dashed arrow) by WTET in synaptic input S2 1 h after pSTDP induction resulted in a statistically significant potentiation in S2 that lasted for 3 h after the WTET ($n = 11$). (*B*) Experiment design is similar to that in *A*. Instead of WTET, a "weak" pSTDP was induced in synaptic input S2 by pairing of pre- (S2) and postsynaptic (S0) pathway stimulations at 40 ms (blue arrow). Both inputs S1 and S2 displayed statistically significant potentiation until the end of the recording ($n = 6$). (*C*) pSTDP was induced in synaptic input S1 (red circles) by pairing (solid arrow) of simultaneous stimulations of pre- (S1) and postsynaptic (S0) pathways. Thirty minutes after pairing, WLFS (dotted arrow) was delivered to an independent synaptic input S2 (blue circles). Input S2 showed an immediate decrease in fEPSPs which returned to baseline level by the end of the recording ($n = 7$). (*D*) Persistent potentiation was observed in input S1 (red circle) for 4 h after the induction of late LTP by three consecutive trains of high-frequency tetanization (STET; small solid arrows). Subsequently, 30 min after the onset of STET, WLFS (dotted arrow) was delivered to a separate synaptic input S2 (blue circles). This resulted in a stable depression in S2 that was statistically significant throughout the experiment ($n = 7$). (*E*) WLFS (dotted arrow) resulted in a transient depression in input S1 (red circles) that reverted to baseline level within 220 min. Thirty minutes after the onset of WLFS, pSTDP was induced in synaptic input S2 (blue circles) by pairing of simultaneous stimulations of presynaptic (S2) and postsynaptic (S0) pathways; this led to a statistically significant potentiation in input S2 that maintained until the end of the recording ($n = 6$). (*F*) A stable depression was observed in input S1 (red circles) from immediately after WLFS (dotted arrow) until the end of the recording. On another independent pathway S2 (blue circles), STET (small solid arrows) was delivered 30 min after the onset of WLFS. This led to a stable potentiation that was statistically significant throughout the recording ($n = 7$). All data show mean ± SEM. Analog traces show representative fEPSPs at 15 min before (S1 and S2: black dashed lines), 30 min after (S1: orange dashed line; S2: turquoise dashed line), and 240 min after (S1: red solid line; S2: blue solid line) the first induction of synaptic plasticity. (Scale bars for analog traces in *A*–*F*: 3 mV/5 ms.)

significant until 220 min (Fig. 6*E*, red circles; $n = 6$; at +220 min, normalized fEPSP = 89.98 ± 3.34%; +220 min vs. −15 min, Wilcox test, $P = 0.03$). Thirty minutes after the start of WLFS, pSTDP was induced in an independent pathway S2 by repeated pairing of simultaneous alveus S0 and presynaptic pathway S2 stimulations. This resulted in a statistically significant potentiation in S2 that lasted until the end of the recording (Fig. 6*E*, blue circles; at +240 min, normalized fEPSP = 128.8 ± 2.29%; +240 min vs. −15 min, Wilcox test, $P = 0.03$). In contrast, persistent LTD was observed when WLFS preceded late-LTP induction by 30 min (Fig. 6*F*). A stable homosynaptic depression was observed for 4 h after WLFS induction in synaptic input S1 (Fig. 6*F*, red circles; $n = 6$; at +240 min, normalized fEPSP = 72.51 ± 1.69%; +240 min vs. −15 min, Wilcox test, $P = 0.02$). STET was delivered to synaptic pathway S2 30 min after WLFS onset, and this led to a persistent LTP in S2 throughout the recording (Fig. 6*F*, blue circles; at +240 min, normalized fEPSP = 143.5 ± 9.09%; +240 min vs. −15 min, Wilcox test, $P = 0.02$).

Discussion

Our study demonstrates that STDP can be induced in a population of SC-CA1 synapses in acute rat hippocampal slices by repeated pairing of presynaptic stimulation and antidromically induced population spike. A small number of repeats (20 pairs of costimulations) at a low frequency (1 Hz) was sufficient to elicit persistent changes in synaptic efficacy that lasted for as long as 4 h. Such a long duration of recording had not been reported in previous studies of STDP, which employed whole-cell voltage clamping or optical imaging experiments that typically lasted for less than 90 min (13, 15, 18–20). Importantly, our prolonged recordings revealed that, in addition to the initial change in magnitude of synaptic strength, the long-term persistence and maintenance of synaptic change also vary as a function of the timing interval between pre- and postsynaptic activities.

By pairing the s.r. and the alveus stimulations, we timed the presynaptic glutamate release with an independent postsynaptic depolarization event at various intervals. As aforementioned, this simulates possible depolarization of CA1 neurons due to ongoing neuronal network activity. Although the extracellular stimulation of the various pathways admittedly allows less precise control over the spike timing of the CA1 pyramidal neurons, we were still able to observe a strong dependency of the strength and persistence of pathway-specific synaptic modification on the temporal sequence and timing of pre- and postsynaptic activities. Furthermore, we conducted these experiments without additional interference of the neuronal network due to inhibition of GABAergic or glial systems, as it was necessary in the previously mentioned whole-cell voltage-clamp studies. Even in the presence of intact inhibitory circuits (22, 23) or glial cells that were most likely activated by the antidromic stimulation (24) in the CA1 region, the pSTDP timing dependency remained similar to that in whole-cell voltage-clamp studies. In general, inhibitory circuits and glial cells that dynamically respond to CA1 pyramidal neuron activity might present a third factor that influences pSTDP (19, 23, 25). Nevertheless, this presumably resembles a physiological situation in which multiple CA1 principle neurons would be active concurrently and their concomitant activity could influence feedforward and feedback microcircuits in the CA1 region (26). Our results present how excitatory and inhibitory connections integrate within the hippocampal CA1 network and regulate synaptic plasticity at SC-CA1 synapses in a timing-dependent manner.

Furthermore, we observed that pSTDP was dependent upon mRNA translation. This observation implies that even a small number of near-coincidental pre- and postsynaptic activities is sufficient to trigger the synthesis of PRPs. This stands in contrast to the convention that repeated tetanic trains are necessary for protein synthesis-dependent LTP (27). In addition, these newly synthesized PRPs could presumably be available at nearby synapses that received insufficient synaptic activity to express lasting synaptic potentiation by themselves but were still able to express a synaptic "tag." Thus, by capturing and utilizing the PRPs synthesized in response to pSTDP induction, a transient weak LTP was transformed into a lasting one. These results suggest that the basic mechanisms of STC are shared between potentiation induced by pairing protocols and conventional tetanization-induced LTP. Furthermore, the result that a "strong" pSTDP could reinforce a "weak" pSTDP into a long-lasting potentiation suggests that pairing at 40 ms led to the setting of synaptic tags without inducing PRPs synthesis by itself. In view of this, the shift in pSTDP curve over time (depicted in Fig. 4) could be interpreted as an indicator of the efficacy of particular activity patterns in setting synaptic tags and inducing PRPs synthesis: Pairing pre- and postsynaptic stimulations at a relative timing interval of $-10 \text{ ms} \leq \Delta t < 30 \text{ ms}$ led to both tag setting and PRP synthesis, while pairing at $\Delta t \geq 30$ ms only led to the setting of transient synaptic tags.

On the contrary, pSTDP induced in one synaptic pathway could not support the maintenance of pathway-specific LTD induced by a low-frequency stimulation protocol on a separate pathway. Interestingly, this suggests that the set of PRPs induced by our pairing protocol is process-specific as it only reinforced LTP but not LTD. This is strikingly different from the cross-tagging phenomenon observed with tetanization-induced LTP, in which high-frequency stimulation triggers the synthesis of PRPs that could support both LTP and LTD (3, 10). A transformation of synaptic transmission by spike-timing-dependent mechanisms could further enhance input-specific information processing, probably through more localized and process-specific protein synthesis. Nevertheless, it has been demonstrated that BDNF is required for the transformation of early LTD into late LTD in cross-tagging (11). However, our results suggest that pSTDP does not require BDNF release (discussed below with further elaboration). The lack of BDNF contribution in pSTDP could underlie the absence of cross-tagging between pSTDP and LFS-LTD.

We have shown that pSTDP required functional CaMKII, NMDA receptors, and de novo protein synthesis and that pSTDP engaged in STC. These results indirectly suggest postsynaptic mechanisms of expression of pSTDP. Pre- and postsynaptic activity pairs elicit calcium transients through NMDA receptors and other calcium channels in the postsynaptic neuron. Varying calcium dynamics, determined by the order and temporal difference between presynaptic and postsynaptic stimulations (19), activates downstream signaling cascades, for example the CaMKII-dependent pathway, to different degrees, thus resulting not only in differences in initial synaptic modification but also differences in the endurance of the evoked synaptic state.

Interestingly, when postsynaptic stimulation preceded presynaptic stimulation by 20 ms, a slight potentiation was observed immediately; yet, the potentiation was not sustained and gradually transformed into a stable depression around 3 h after pSTDP induction. A possible interpretation is that this pattern of activity concomitantly triggered local synaptic state changes for potentiation and set covert tags for depression. The tags for depression were masked by the immediate changes that transiently increased synaptic transmission. However, it appears that only the tags for depression captured newly synthesized PRPs, while the synaptic changes that support potentiation gradually waned; hence, a lasting weakening of the synapses was reinforced. Wang et al. (28) showed that specific spike patterns can concurrently activate potentiation and depression processes, which integrate nonlinearly in a timing-dependent fashion. Furthermore, as mentioned above, conventional LTP and LTD rely on tags of different kinase signaling cascades (29), even though some PRPs are shared between LTP and LTD (3). Therefore, it

seems plausible that cellular mechanisms for potentiation and depression were activated concurrently, yet to various degrees, by specific pSTDP induction patterns. These processes integrated, modified the activated synapses on different time scales, and manifested in synaptic states that morphed gradually. However, the exact molecular mechanisms involved remain to be investigated.

In the study of the possible involvement of BDNF in pSTDP, the hippocampal slices were perfused with TrkB-Fc 30 min before and 30 min after the pSTDP induction. This treatment presumably depletes constitutively released extracellular BDNF and those, if any, newly secreted in response to activity induction. pSTDP expression was not eliminated by TrkB-Fc application, suggesting that BDNF does not play a key role in pSTDP in our preparation. These results stand in contrast to some earlier studies (30, 31) but are in broad agreement with other reports on the involvement of this neurotrophin in STDP. Edelmann et al. (32) reported that blocking BDNF/TrkB signaling had no effect on STDP induced by canonical 1:1 pairing but impaired STDP induced by 1:4 pairing of presynaptic and postsynaptic stimulations. Also, a pairing-induced release of BDNF from cultured hippocampal neurons was dependent on the number of pairs of glutamate-spike stimulation (33): A minimum of 40 to 80 pairs of stimuli was required to induce spike-timing-dependent secretion of BDNF, while 20 pairs did not lead to a detectable release of BDNF from dendritic spines. Our results corroborate these earlier findings that BDNF requirement and release in STDP are dependent on the activity pattern—specifically, BDNF is unnecessary for STDP induced by a low number of paired, single pre- and postsynaptic activities.

On a similar note, we also observed dependence of pSTDP expression on the number of pre- and postsynaptic stimuli pairs, although only one timing interval was tested. However, how the number of pairings influences the full pSTDP curve and its physiological implications on CA1 network functions remain a topic for future studies.

In summary, near-synchronous pre- and postsynaptic activity was sufficient to trigger long-lasting changes in synaptic efficacy in a group of CA3–CA1 synapses. Specifically, we showed that the long-term endurance of synaptic modifications varied as a function of the order and timing between pre- and postsynaptic activities. In addition, we showed that pSTDP induction leads to the synthesis of PRPs that also strengthen weak LTP and weak pSTDP on other synapses. Thus, a low number of low-frequency concomitant pre- and postsynaptic events of interconnected CA3 and CA1 neurons is able to drastically increase the potential of modulation of synaptic transmission. Significantly, we demonstrated that STDP lasts for many hours. Corroborating previous publications, this highlights the importance of STDP-related mechanisms in achieving synaptic plasticity under physiological conditions.

Materials and Methods

Acute hippocampal slices prepared from male Wistar rats (P35–49) were used for electrophysiological experiments. All experimental procedures were approved by the Institutional Animal Care and Use Committee of the National University of Singapore. Further details about slice preparation, field electrophysiology and whole-cell patch-clamp experiments, pharmacology, and statistical analysis are provided in *SI Appendix*.

ACKNOWLEDGMENTS. We thank Ms. Sheila Ang and Mr. Chong Yee Song for their constructive comments. This work was supported by National Medical Research Council Collaborative Research Grants NMRC/CBRG/0099/2015 and NMRC-OFIRG-0037-2017 (to K.K.L.P., M.S, K.K.-K., and S.S.), National University of Singapore Strategic and Aspiration Research Funds, and Ministry of Education Academic Research Fund Tier 3 Grant MOE2017-T3-1-002. T.B. is supported by Natural Science Foundation of China Grants 31320103906 and 31871076. The funder had no role in study design, data collection, or interpretation.

1. Takeuchi T, Duszkiewicz AJ, Morris RG (2013) The synaptic plasticity and memory hypothesis: Encoding, storage and persistence. *Philos Trans R Soc Lond B Biol Sci* 369: 20130288.
2. Frey U, Huang YY, Kandel ER (1993) Effects of cAMP simulate a late stage of LTP in hippocampal CA1 neurons. *Science* 260:1661–1664.
3. Sajikumar S, Navakkode S, Sacktor TC, Frey JU (2005) Synaptic tagging and cross-tagging: The role of protein kinase Mzeta in maintaining long-term potentiation but not long-term depression. *J Neurosci* 25:5750–5756.
4. Nguyen PV, Woo NH (2003) Regulation of hippocampal synaptic plasticity by cyclic AMP-dependent protein kinases. *Prog Neurobiol* 71:401–437.
5. Yang SN, Tang YG, Zucker RS (1999) Selective induction of LTP and LTD by postsynaptic [Ca2+]i elevation. *J Neurophysiol* 81:781–787.
6. Navakkode S, Sajikumar S, Frey JU (2004) The type IV-specific phosphodiesterase inhibitor rolipram and its effect on hippocampal long-term potentiation and synaptic tagging. *J Neurosci* 24:7740–7744.
7. Shivarama Shetty M, Sajikumar S (2017) 'Tagging' along memories in aging: Synaptic tagging and capture mechanisms in the aged hippocampus. *Ageing Res Rev* 35:22–35.
8. Frey U, Morris RG (1997) Synaptic tagging and long-term potentiation. *Nature* 385: 533–536.
9. Redondo RL, Morris RG (2011) Making memories last: The synaptic tagging and capture hypothesis. *Nat Rev Neurosci* 12:17–30.
10. Sajikumar S, Frey JU (2004) Late-associativity, synaptic tagging, and the role of dopamine during LTP and LTD. *Neurobiol Learn Mem* 82:12–25.
11. Sajikumar S, Korte M (2011) Metaplasticity governs compartmentalization of synaptic tagging and capture through brain-derived neurotrophic factor (BDNF) and protein kinase Mzeta (PKMzeta). *Proc Natl Acad Sci USA* 108:2551–2556.
12. Markram H, Lübke J, Frotscher M, Sakmann B (1997) Regulation of synaptic efficacy by coincidence of postsynaptic APs and EPSPs. *Science* 275:213–215.
13. Bi GQ, Poo MM (1998) Synaptic modifications in cultured hippocampal neurons: Dependence on spike timing, synaptic strength, and postsynaptic cell type. *J Neurosci* 18: 10464–10472.
14. Buchanan KA, Mellor JR (2010) The activity requirements for spike timing-dependent plasticity in the hippocampus. *Front Synaptic Neurosci* 2:11.
15. Campanac E, Debanne D (2008) Spike timing-dependent plasticity: A learning rule for dendritic integration in rat CA1 pyramidal neurons. *J Physiol* 586:779–793.
16. Pike FG, Meredith RM, Olding AW, Paulsen O (1999) Rapid report: Postsynaptic bursting is essential for 'Hebbian' induction of associative long-term potentiation at excitatory synapses in rat hippocampus. *J Physiol* 518:571–576.
17. Nishiyama M, Hong K, Mikoshiba K, Poo MM, Kato K (2000) Calcium stores regulate the polarity and input specificity of synaptic modification. *Nature* 408:584–588.
18. Wittenberg GM, Wang SSH (2006) Malleability of spike-timing-dependent plasticity at the CA3-CA1 synapse. *J Neurosci* 26:6610–6617.
19. Aihara T, et al. (2007) The relation between spike-timing dependent plasticity and Ca2+ dynamics in the hippocampal CA1 network. *Neuroscience* 145:80–87.
20. Meredith RM, Floyer-Lea AM, Paulsen O (2003) Maturation of long-term potentiation induction rules in rodent hippocampus: Role of GABAergic inhibition. *J Neurosci* 23: 11142–11146.
21. Leung LW (1979) Potentials evoked by alvear tract in hippocampal CA1 region of rats. I. Topographical projection, component analysis, and correlation with unit activities. *J Neurophysiol* 42:1557–1570.
22. Pouille F, Scanziani M (2004) Routing of spike series by dynamic circuits in the hippocampus. *Nature* 429:717–723.
23. Nishiyama M, Togashi K, Aihara T, Hong K (2010) GABAergic activities control spike timing- and frequency-dependent long-term depression at hippocampal excitatory synapses. *Front Synaptic Neurosci* 2:22.
24. Hulme SR, Jones OD, Raymond CR, Sah P, Abraham WC (2013) Mechanisms of heterosynaptic metaplasticity. *Philos Trans R Soc Lond B Biol Sci* 369:20130148.
25. Valtcheva S, Venance L (2016) Astrocytes gate Hebbian synaptic plasticity in the striatum. *Nat Commun* 7:13845.
26. English DF, et al. (2017) Pyramidal cell-interneuron circuit architecture and dynamics in hippocampal networks. *Neuron* 96:505–520.e7.
27. Huang YY, Kandel ER (1994) Recruitment of long-lasting and protein kinase A-dependent long-term potentiation in the CA1 region of hippocampus requires repeated tetanization. *Learn Mem* 1:74–82.
28. Wang HX, Gerkin RC, Nauen DW, Bi GQ (2005) Coactivation and timing-dependent integration of synaptic potentiation and depression. *Nat Neurosci* 8:187–193.
29. Sajikumar S, Navakkode S, Frey JU (2007) Identification of compartment- and process-specific molecules required for "synaptic tagging" during long-term potentiation and long-term depression in hippocampal CA1. *J Neurosci* 27:5068–5080.
30. Tanaka J, et al. (2008) Protein synthesis and neurotrophin-dependent structural plasticity of single dendritic spines. *Science* 319:1683–1687.
31. Mu Y, Poo MM (2006) Spike timing-dependent LTP/LTD mediates visual experience-dependent plasticity in a developing retinotectal system. *Neuron* 50:115–125.
32. Edelmann E, et al. (2015) Theta burst firing recruits BDNF release and signaling in postsynaptic CA1 neurons in spike-timing-dependent LTP. *Neuron* 86:1041–1054.
33. Lu H, Park H, Poo MM (2013) Spike-timing-dependent BDNF secretion and synaptic plasticity. *Philos Trans R Soc Lond B Biol Sci* 369:20130132.